Modeling driving behavior and traffic flow at sags

Bernat Goñi Ros*, Victor L. Knoop, Bart van Arem, Serge P. Hoogendoorn
Delft University of Technology
Faculty of Civil Engineering and Geosciences
Department of Transport and Planning
Stevinweg 1, 2628CN, Delft, The Netherlands
* Corresponding author. E-mail address: b.goniros@tudelft.nl

ABSTRACT

Sags are freeway sections along which gradient changes significantly from downwards to upwards. Sags are often bottlenecks in freeway networks. Capacity decreases due to changes in car-following behavior. We present a microscopic traffic flow model that describes driving behavior and traffic flow dynamics at sags. The model includes a new longitudinal driving behavior model that accounts for the fact that drivers generally have a limited ability to compensate for the negative effect that an increase in slope has on vehicle acceleration. The face-validity of the microscopic model is tested by means of a simulation study. The study site is a sag of the Tomei Expressway (near Tokyo). The simulation results are compared to empirical findings presented in the literature. We show that the model is capable of reproducing all the relevant phenomena that cause the formation of congestion at sags.

Keywords: Sag, Congestion, Microscopic Traffic Flow Model, Model Face-Validity

1. INTRODUCTION

Sags are freeway sections along which the road gradient changes significantly from downwards to upwards in the direction of traffic [1]. The traffic flow capacity of sags is generally lower than that of flat sections [2, 3]. Because of that, sags often become bottlenecks in freeway networks. In order to evaluate the effectiveness of possible control measures to reduce congestion at sags, it is necessary to model traffic flow dynamics at that type of bottlenecks in a sufficiently realistic way. In this paper, we present a microscopic traffic flow model that aims to reproduce the phenomena causing the formation of congestion at sags. The model has five sub-models: 1) network model; 2) traffic demand model; 3) longitudinal driving behavior model; 4) lateral driving behavior models; and 5) traffic composition model. The main novelty of our microscopic traffic flow model is the longitudinal driving behavior modeling approach. We propose a new approach that accounts for the fact that drivers have a limited ability to compensate for the negative effect that an increase in slope has on vehicle acceleration. The face-validity of the microscopic traffic flow model is tested by means of a simulation study. The study site is the Yamato sag (Tomei

Expressway, near Tokyo). The traffic flow patterns obtained from simulation are compared to the patterns observed in real freeways according to the scientific literature. We show that the proposed microscopic traffic flow model is capable of reproducing all the relevant phenomena that cause the formation of congestion at sags.

2. CAUSES OF CONGESTION AT SAGS: EMPIRICAL EVIDENCE

Various empirical studies show that traffic flow capacity can be significantly lower at sags than at flat sections having the same number of lanes (even 30% lower) [2, 3]. Because of that, sags often become bottlenecks in freeway networks, causing the formation of congestion in conditions of high traffic demand. In general, the lower part of the uphill section (i.e., first 500-1000 m downstream of the bottom of the sag) is the main bottleneck [4]. The factors reducing the capacity of the uphill section at sags appear to be related primarily to two changes in car-following behavior that occur when vehicles reach the uphill section. First, drivers tend to reduce speed [1, 2, 4, 5]. Second, drivers tend to keep longer headways than expected given their speed [5, 6, 7]. These two changes in car-following behavior have a negative effect on the capacity of the uphill section: traffic flow becomes congested at lower flow rates than on flat sections [2, 5]. The above-mentioned changes in car-following behavior seem to be unintentional [6]. They are caused by a limitation in vehicle acceleration resulting from the combination of two factors: i) increase in resistance force; and ii) insufficient acceleration operation by drivers [2, 6]. Drivers fail to accelerate sufficiently even though they generally perceive the change in gradient [1, 6]. The reason why drivers do not accelerate sufficiently on the lower part of the uphill section seems to be related to their throttle operation behavior: drivers generally push down the throttle pedal at the beginning of the uphill section but it takes time for them to adapt the throttle position and compensate for the increase in resistance force [6]. Drivers are generally able to re-accelerate after the first 500-1000 m of the uphill section and recover their desired speed [6].

Typically, the process of congestion formation at sags has two phases. First, congestion forms on the median lane of the uphill section [2, 8, 9]. The main reason why congestion emerges first on the median lane is related to an uneven lane flow distribution: with high demand and uncongested traffic, flows tend to be higher (and closer to capacity) on the median lane than on the other lanes [2, 8, 10]. Second, congestion spreads from the median lane to the other lanes [2, 8, 9]. When flow becomes congested on the median lane, some vehicles migrate from that lane to the less crowded lanes in order to avoid queuing [8, 9]. When flow on those lanes increases above capacity, traffic also breaks down there. At that point, congestion has spread to all lanes, causing a significant decrease in total outflow (due to the *capacity drop* phenomenon) and the formation of a queue upstream of the bottleneck [2, 9, 10].

To summarize, the scientific literature suggests that the most relevant phenomena causing the

formation of congestion at sags are the following: a) changes in car-following behavior on the lower part of the uphill section; b) reduced capacity on the lower part of the uphill section (bottleneck); c) uneven lane flow distribution under conditions of high demand; d) initial occurrence of congestion on the median lane; e) redistribution of vehicles across lanes (by lane changes); f) spreading of congestion to the other lanes; g) capacity drop in congestion; h) queue formation and growth. Any model that aims to reproduce traffic flow dynamics at sags in a realistic way should be capable of reproducing all the phenomena mentioned above.

3. MICROSCOPIC TRAFFIC FLOW MODEL

We developed a microscopic traffic flow model consisting of five sub-models: 1) network model; 2) traffic demand model; 3) longitudinal driving behavior model; 4) lateral driving behavior model; and 5) traffic composition model.

3.1 Network model

The network model describes the characteristics of the freeway network, including: a) number of sections; b) section length; c) degree of gradient along each section; d) number of lanes per section; and e) speed limit per section and lane. Horizontal curves are not taken into account. With regard to gradient, a sag is modeled as a combination of three sections (see Figure 1): 1) constant-gradient downhill section; 2) constant-gradient uphill section; and 3) transition section (i.e., section along which gradient increases linearly from the negative value of the constant-gradient downhill section to the positive value of the constant-gradient uphill section).

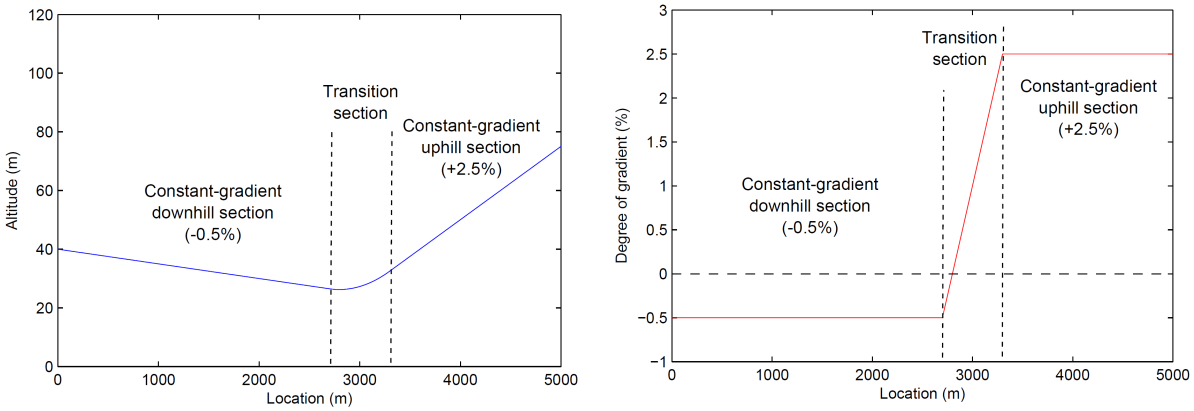

a) Altitude vs. distance b) Degree of gradient vs. distance

Figure 1. Representation of sag by means of three sections (Yamato sag, Tomei Expressway)

3.2 Traffic demand model

The traffic demand model specifies the inflow (vehicles/h) at the network entry point at each time step. Given the total inflow, Q, the inflow per lane, q_i, is calculated based on the lane flow distribution model presented by Wu [11].

3.3 Longitudinal driving behavior model

The longitudinal driving behavior model takes into account the influence of changes in gradient on vehicle acceleration. The model is based on three principles, which are supported by empirical evidence (see Section 2). First, drivers perceive the change in gradient at sags. Second, drivers react to the change in gradient by pushing down the throttle pedal, but they may not be able to fully compensate for the increase in resistance force at the beginning of the uphill section, which limits vehicle acceleration. Third, over time, drivers gradually compensate for the increase in resistance force on the uphill section; hence the negative effect that the change in gradient has on vehicle acceleration decreases over time. In the proposed longitudinal driving behavior model, vehicle acceleration is determined by a two-term additive function. The first term accounts for the influence of speed, relative speed and spacing on vehicle acceleration. It is based on the Intelligent Driver Model (IDM) [12]. We added the second term to account for the effect of changes in gradient on acceleration.

$$\dot{v}(t) = a \cdot \left[1 - \left(\frac{v(t)}{v_{des}(t)} \right)^4 - \left(\frac{s(t)}{s^*(t)} \right)^2 \right] - g \cdot \left[G(t) - G_c(t) \right] \tag{1}$$

where:

$$s^*(t) = s_0 + \gamma \cdot v(t) \cdot T + \frac{v(t) \cdot \Delta v(t)}{2\sqrt{ab}} \tag{2}$$

$$G_c(t) = \begin{cases} G(t) & if \;\; G(t) \le G(t_c) + c \cdot (t - t_c) \\ G(t_c) + c \cdot (t - t_c) & if \;\; G(t) > G(t_c) + c \cdot (t - t_c) \end{cases} \tag{3}$$

In Equations (1) to (3): t is time; v is vehicle speed; Δv is relative speed to the leading vehicle ($\Delta v = v - v_L$, where v_L is the speed of the leading vehicle); s is net distance headway; s^* is desired net distance headway; v_{des} is desired speed (parameter); a is maximum acceleration (parameter); b is desired deceleration (parameter); s_0 is net distance headway at standstill (parameter); T is safe time headway (parameter); γ is a congestion factor on safe time headway that accounts for the capacity drop in congestion ($\gamma = 1$ if $v \ge v_{crit}$, and $\gamma > 1$ if $v < v_{crit}$, where v_{crit} is the critical congestion speed) (γ and v_{crit} are parameters); g is the gravitational acceleration; $G(t)$ is freeway gradient at the location where the vehicle is at time t; $G_c(t)$ is compensated gradient at time t (note that $G_c(t) \le G(t)$); t_c is the time when the driver could no longer fully compensate for the gradient change ($t_c = max(t | G_c(t) = G(t))$); and c is the maximum gradient compensation rate (parameter).

The model takes into account the influence of changes in slope on vehicle acceleration by using the concept of *compensated gradient*. The compensated gradient, G_c, is a variable that accounts for the fact that drivers have a limited ability to accelerate when gradient changes.

The model assumes that drivers compensate for positive changes in slope linearly over time (with a maximum compensation rate defined by parameter *c*). This assumption is based on findings by Yoshizawa *et al.* [6]. Note that the model assumes that drivers can fully compensate for negative changes in gradient.

3.4 Lateral driving behavior model

Lateral driving behavior plays an important role in the process of congestion formation at sags. However, there is no evidence suggesting that lateral driving behavior *changes* at sags. The traffic conditions change when traffic breaks down, which may induce drivers to perform lane-changing maneuvers; but the behavior itself does not seem to change. For that reason, to describe lateral driving behavior at sags, we used an existing model: the *Lane Change Model with Relaxation and Synchronization* (LMRS) [13]. Note that we modified the LMRS regarding the calculation of the speed gain desire incentive: in our lateral driving behavior model, the speed of all leading vehicles that are not farther ahead than x_0 meters has the same weight when calculating the anticipated speed of downstream traffic.

3.5 Traffic composition model

The traffic composition model describes the characteristics of the vehicle and driver populations. The vehicle characteristics taken into account by the model are vehicle length, l, and desired speed, v_{des}. The driver characteristics are related to the parameters of the longitudinal and lateral driving behavior models. For each vehicle type, different types of drivers can be specified, with different parameters. The traffic composition model specifies the percentage of vehicle-driver units within the flow entering the network that belong to each vehicle and driver type. Traffic composition is specified per lane.

4. MODEL VERIFICATION

The face-validity of the proposed microscopic traffic flow model was tested by means of a simulation study, using the Yamato sag (Tomei Expressway, near Yokyo) as study site. In this section, we present the settings and the results of the simulation study.

4.1 Simulation settings

The simulation site is a freeway stretch, 5 km long, with three lanes (median, center and shoulder lanes). The stretch contains a sag with a vertical profile similar to the one of the Yamato sag (Tomei Expressway, near Tokyo) (see Figure 1). The speed limit on all lanes is 100 km/h for cars and 85 km/h for trucks. The simulation period is 100 min. The total flow on all lanes at $x = 0$ increases linearly from $Q = 3000$ veh/h to $Q = 5200$ veh/h between $t = 0$ and $t = 75$ min. From $t = 75$ min to $t = 100$ min, total inflow stays at 5200 veh/h. The lane flow distribution changes over time according to the traffic demand model presented in Section 3.2. For three-lane freeways, we use the same parameter values provided by Wu [11] (see Table 6

of that reference), except for a and e on the center lane (we use a=0.39 and e=0.30). We slightly modified the values of those two parameters to make the lane flow distribution model more accurate for Japanese freeways, based on empirical data presented by Xing *et al.* [10].

Table 1. Parameters of the longitudinal and lateral driving behavior models

Vehicle type	Car	Car	Car	Truck
Driver type	Car driver 1	Car driver 2	Car driver 3	Truck driver
l (m)	4	4	4	15
a_0 (m/s^2)	1.25	1.25	1.25	1.50
b_0 (m/s^2)	1.80	1.80	1.80	1.50
T_0 (s)	1.45	1.20	1.15	1.50
s_0 (m)	3	3	3	3
$v_{des,0}$ (km/h)	100	100	100	
v_{crit} (km/h)	60	60	60	60
c_0 (s^{-1})	0.00042	0.00042	0.00042	0.00042
γ (-)	1.15	1.15	1.15	1.15
δ*(-)	0.92	0.97	1.03	1.00
σ_δ (-)	0.03	0.10	0.10	0.00
$v^*_{des,t}$ (km/h)				85
$\sigma_{vdes,t}$ (km/h)				2.5
$T_{min,0}$ (s)	0.56	0.56	0.56	0.56
τ (s)	25	25	25	25
x_0 (m)	200	200	200	200
v_{gain} (km/h)	70	50	50	70
d^{ij}_{free} (-)	0.365	0.365	0.365	0.365
d^{ij}_{sync} (-)	0.577	0.577	0.577	0.577
d^{ij}_{coop} (-)	0.788	0.788	0.788	0.788

We defined two different types of vehicles: cars and trucks. Also, we defined three types of car drivers (each corresponding to one lane) and one type of truck driver. Defining one car driver type per lane was necessary to take into account the differences in desired speed and car-following behavior between lanes observed in empirical traffic data [9]. The parameters of the longitudinal and lateral driving behavior models are shown in Table 1. For the interpretation of the lateral driving behavior model parameters, we refer to Schakel *et al.* [13]. We included stochasticity in some parameters of the longitudinal and lateral driving behavior models (v_{des}, a, b, T, c, T_{min} for car drivers, and v_{des} for truck drivers). The value of those parameters differs between drivers belonging to the same driver type. For car drivers, those parameters depend on the stochastic factor δ, which differs between drivers (it is Gaussian

distributed with mean δ^* and standard deviation σ_δ): $v_{des} = \delta \cdot v_{des,0}$; $a = \delta \cdot a_0$; $b = \delta \cdot b_0$; $T = T_0/\delta$; $c = \delta \cdot c_0$; and $T_{min} = T_{min,0}/\delta$. For trucks, only the desired speed parameter is considered to be stochastic. That parameter is assumed to be Gaussian distributed with mean $v^*_{des,t}$ and standard deviation $\sigma_{vdes,t}$. The composition of traffic entering the network is shown in Table 2.

Table 2. Traffic composition

Vehicle type	Car	Car	Car	Truck
Driver type	Car driver 1	Car driver 2	Car driver 3	Truck driver
Shoulder lane	90%	0%	0%	10%
Center lane	0%	95%	0%	5%
Median lane	0%	0%	100%	0%

4.2 Simulation results

The simulation results show that traffic breaks down at the sag of the study site a little bit before t = 75 min = 4500 s, when total traffic demand is approaching 5200 veh/h (see Figures 2 and 3c). The end of the transition section constitutes the bottleneck (Figure 2). The process of congestion formation is the following: 1) congestion occurs on the median lane (Figures 2 and 3a); 2) some drivers move from the median lane to the other lanes, and as a consequence flow on the center and shoulder lanes increases (Figure 3b); 3) traffic breaks down on those lanes as well (Figures 2 and 3a). The occurrence of congestion on a lane results in reduced lane flow, due to the capacity drop phenomenon (Figure 3b). When congestion has spread to all lanes, the total outflow at the bottleneck is about 5000 veh/h, i.e., 4% lower than the total inflow upstream of the bottleneck (Figure 3c), and a queue of vehicles forms upstream of the bottleneck. On all lanes, the head of the queue stays at the end of the transition section (Figure 2). No collisions between vehicles occurred during the simulations.

4.3 Model verification

The traffic flow patterns obtained from simulation are similar to the patterns observed in real freeways. The microscopic traffic flow model is capable of reproducing all the relevant phenomena that cause the formation of congestion at sags, which are described in Section 2. The capacity of the lower part of the uphill section decreases due to the changes in car-following behavior resulting from the limiting effect that the change in slope has on vehicle acceleration. The main bottleneck is the end of the transition section, where vehicle acceleration limitation is stronger (because the difference between actual gradient and compensated gradient is higher). Congestion occurs first on the median lane (because in conditions of high traffic demand, flow is closer to capacity on that lane than on the other lanes). Then, some drivers move from the median lane to the other lanes in order to avoid queuing. As a consequence of these lane changes, flow on the center and shoulder lanes

increases. When the flow on those lanes becomes higher than their capacity, traffic breaks down there, too. The occurrence of congestion on a lane results in reduced lane outflow (due to the capacity drop phenomenon) and the formation of a vehicular queue.

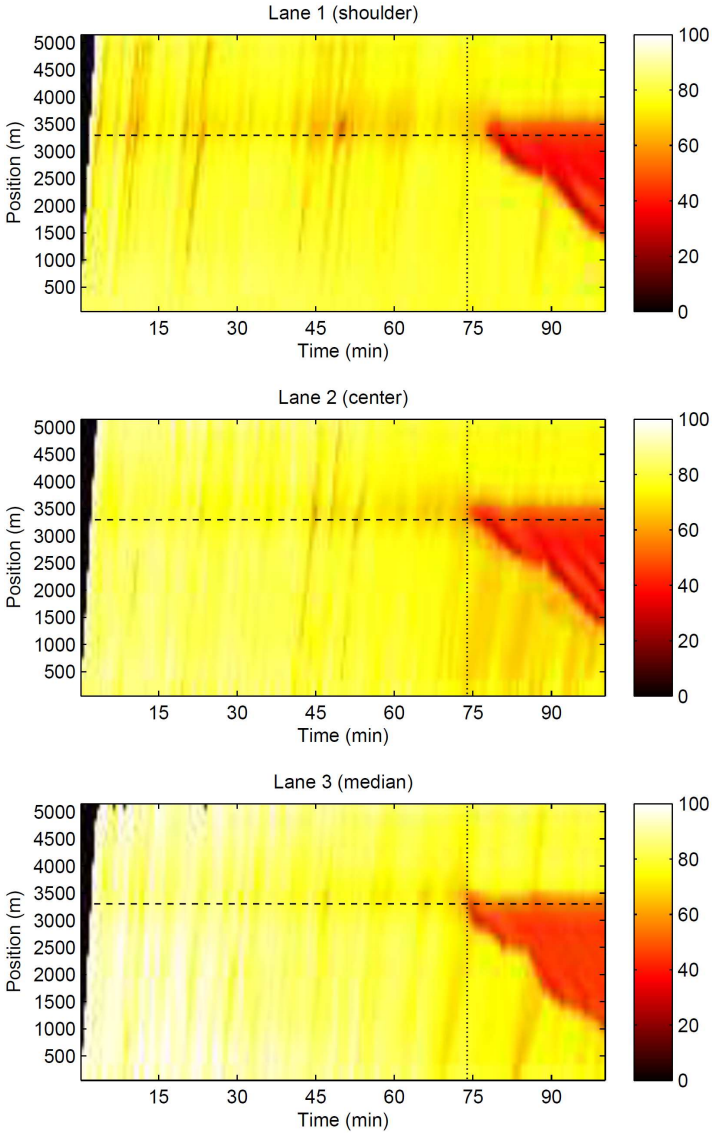

Figure 2. Speed contour plots (the color indicates the speed (km/h), the black dotted lines show the time at which traffic breaks down on the median lane, and the black dashed lines indicate the location at which the transition section ends)

5. CONCLUSIONS

The aim of this paper was to develop a model capable of reproducing traffic flow dynamics at sags in a realistic way. We developed a microscopic traffic flow model consisting of five sub-models: 1) network model; 2) traffic demand model; 3) longitudinal driving behavior model; 4) lateral driving behavior model; and 5) traffic composition model. The face-validity of the proposed model was tested by means of a simulation study. A sag of the Tomei Expressway (near Tokyo) was used as study site. The traffic flow patterns obtained from

simulation were compared to the patterns observed in real freeways (based on data presented in the scientific literature). The simulation results show that the proposed model is capable of reproducing all the relevant traffic flow phenomena that cause the formation of congestion at sags. However, the microscopic traffic flow model still needs to be calibrated and validated, which requires a quantitative comparison of the model output with empirical traffic data. Vehicle trajectory data from the Yamato sag (Tomei Expressway) are available (see [7]), and could be used for calibration and validation of the microscopic traffic flow model. There are various calibration and validation methods; further research should reveal what method should be used in this case. After calibration and validation, the model will be used to evaluate the effectiveness of possible control measures to mitigate congestion at sags.

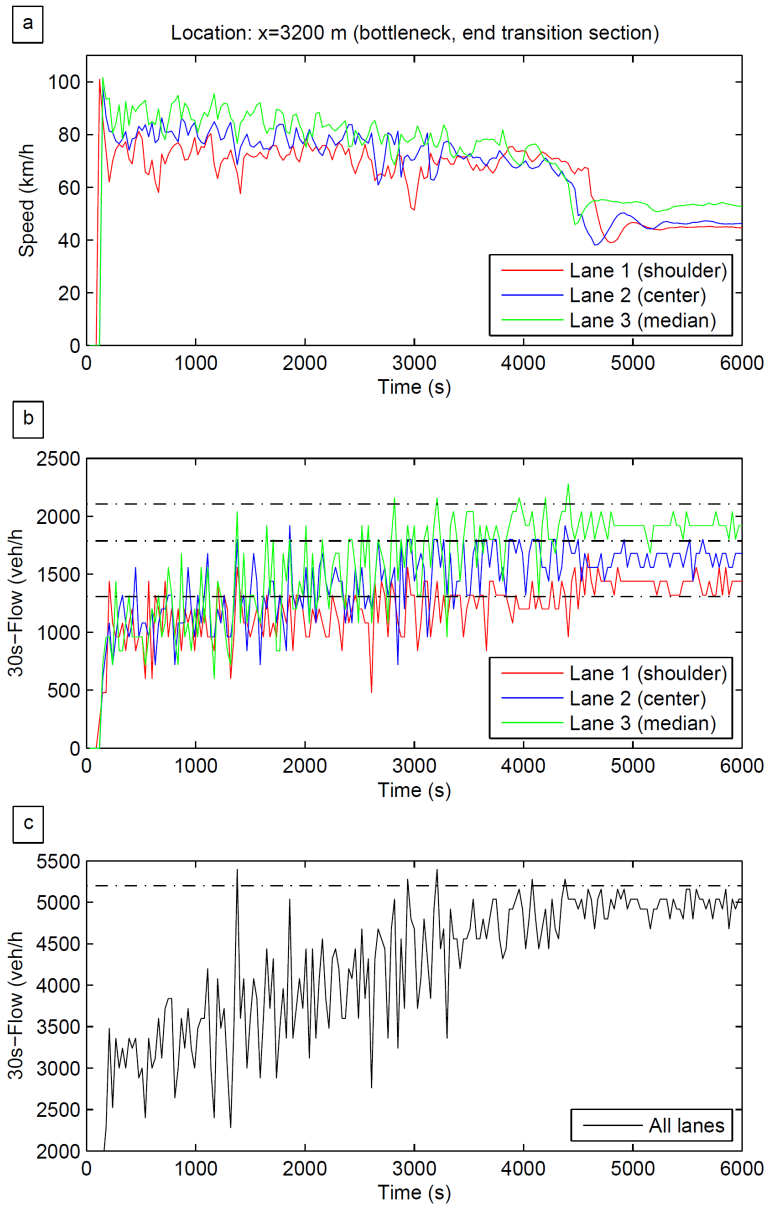

Figure 3. Speeds and flows over time at x=3200 m (the black dashed lines show the average inflow at x=0 m after t= 75 min)

6. ACKNOWLEDGMENT

This research was sponsored by Toyota Motor Europe.

7. REFERENCES

[1] Furuichi, T, Yamamoto, S, Kotani, M and Iwasaki, M, “Characteristics of spatial speed change at motorway sag sections and capacity bottlenecks” in *Proceedings of Annual Meeting of the Transportation Research Board* (Washington, DC, January 2003).

[2] Koshi, M, Kuwahara, M and Akahane, H, “Capacity of sags and tunnels on Japanese motorways”, *ITE Journal*, vol. 62, no. 5, 1992, pp. 17–22.

[3] Okamura, H, Watanabe, S and Watanabe, T, “An empirical study on the capacity of bottlenecks on the basic suburban expressway sections in Japan” in *Proceedings of International Symposium on Highway Capacity* (Maui, Hawaii, June-July 2000).

[4] Brilon, W and Bressler, A, “Traffic flow on freeway upgrades”, *Transportation Research Record: Journal of the Transportation Research Board*, vol. 1883, 2004, pp. 112–121.

[5] Koshi, M, “An Interpretation of a Traffic Engineer on Vehicular Traffic Flow”, *Traffic and Granular Flow’01*, Berlin, Springer, 2001, pp. 199–210.

[6] Yoshizawa, R, Shiomi, Y, Uno, N, Iida, K and Yamaguchi, M, “Analysis of car-following behavior on sag and curve sections at intercity expressways with driving simulator”, *Int. Journal of Intelligent Transportation Systems Research*, vol. 10, no. 2, 2011, pp. 56–65.

[7] Goñi Ros, B, Knoop, V L, van Arem, B and Hoogendoorn, S P, “Car-following Behavior at Sags and its Impacts on Traffic Flow” in *Proceedings of Annual Meeting of the Transportation Research Board* (Washington, DC, January 2013).

[8] Hatakenaka, H, Hirasawa, T, Yamada, K, Yamada, H, Katayama, Y and Maeda, M, “Development of AHS for traffic congestion in sag sections”, *Proceedings of ITS World Congress*, (London, UK, October 2006).

[9] Patire, A D and Cassidy, M J, “Lane changing patterns of bane and benefit: Observations of an uphill expressway”, *Transportation Research Part B: Methodological*, vol. 45, no. 4, 2011, pp. 656–666.

[10] Xing, J, Sagae, K and Muramatsu, E, “Balance lane use of traffic to mitigate motorway traffic congestion with roadside variable message signs”. *Proceedings of ITS World Congress* (Busan, South Korea, October 2010).

[11] Wu, N, “Equilibrium of lane flow distribution on motorways”, *Transportation Research Records: Journal of the Transportation Research Board*, vol. 1965, 2006, pp. 48–59.

[12] Treiber, M, Hennecke, A and Helbing, D, “Congested traffic states in empirical observations and microscopic simulations”, *Physical Review E*, vol. 62, no. 2, 2000, pp. 1805-1824.

[13] Schakel, W, Knoop, V L and van Arem, B, “LMRS: An integrated lane change model with relaxation and synchronization”. *Proceedings of Annual Meeting of the Transportation Research Board* (Washington, DC, January 2012).